

EXAFS study of local order in the amorphous chalcogenide semiconductor $\text{Ge}_2\text{Sb}_2\text{Te}_5$

M. A. PAESLER^{*}, D. A. BAKER, G. LUCOVSKY, A. E. EDWARDS^a, P. C. TAYLOR^b

Physics Department, North Carolina State University, Raleigh, NC 27695-8202

^a*Air Force Research Laboratory, KAFB, NM 87117-5776*

^b*Physics Department, Colorado School of Mines, Golden, CO 80401*

Studies of amorphous (a-) semiconductors have been driven by technological advances as well as fundamental theories. Observation of electrical switching, for example, fueled early interest in a-chalcogenides. More recently switching of the a-chalcogenide $\text{Ge}_2\text{Sb}_2\text{Te}_5$ has been applied quite successfully to DVD technology where the quest for the discovery of better-suited materials continues. Thus, switching provides researchers today with an active arena of technological as well as fundamental study. On the theoretical front, bond constraint theory – or BCT - provides a powerful framework for understanding the structure and properties of a-materials. Applications of BCT to switching in $\text{Ge}_2\text{Sb}_2\text{Te}_5$ holds the promise of finding the best composition suited for switching applications. This work presents EXAFS data that describe local bonding configurations in as-deposited $\text{Ge}_2\text{Sb}_2\text{Te}_5$. The data show that $\text{Ge}_2\text{Sb}_2\text{Te}_5$ may best be viewed as a random array of Ge_2Te_3 and Sb_2Te_3 structural units imbedded in a tissue of a-Te, 17% of which is over-coordinated. In addition, a valence alternation pair defect is introduced to the model to satisfy charge conservation constraints.

(Received November 2, 2006; accepted November 2, 2006)

Keywords: $\text{Ge}_2\text{Sb}_2\text{Te}_5$, Local order, EXAFS, Chalcogenide, Switching material

1. Introduction

The authors are delighted to be given the opportunity to contribute to this Festschrift in honor of the many contributions to investigations of amorphous semiconductors made by Professor Radu Grigorvici. His insights and understanding of the properties of these materials have helped to add a sense of ordered understanding to the study of disordered materials.

Electronic switching [1] in the chalcogenide alloy $\text{Ge}_2\text{Sb}_2\text{Te}_5$ (GST) lies at the heart of existing technologies (DVD memory) while also holding the promise of future devices (PRAM, reconfigurable interconnects, etc.) [2]. Although all of these GST applications rely on property changes associated with an amorphous-crystalline GST transition, a description of the transition itself is a matter of some contention [3, 8]. The present study uses bond constraint theory [4,5,6,7] to provide insights about this transition. Based on Extended X-ray Absorption Fine Structure (EXAFS) data taken on as-deposited samples of GST, the work describes bonding statistics in the random GST network and identifies specific local configurations. The following paragraphs describe experimental results and present an approach to their interpretation based on bond constraint theory, or BCT. The paper continues with a discussion of the role of specific bonding configurations in the crystallization and amorphization processes.

2. Experimental results

EXAFS measurements of as-deposited amorphous GST samples and the subsequent initial analysis are described elsewhere [8]. Table 1 presents a summary of

these results. Nearest neighbor (N) determinations indicate slightly under-coordinated Ge with $N_{\text{Ge}} = 3.9 \pm 0.8$ and slightly over coordinated Sb with $N_{\text{Sb}} = 3.3 \pm 0.6$ and Te with $N_{\text{Te}} = 2.4 \pm 0.6$. Note that the reported bond lengths agree with tabulated covalent radii for each species [9]. The results are shown to be internally consistent for several reasons. First, the Te nearest neighbor distances ($R_{\text{Te-Sb}} = 2.83 \text{ \AA}$ and $R_{\text{Te-Ge}} = 2.62 \text{ \AA}$) are found to be the same, within the error, regardless of whether they were determined from Te-edge data or from the neighboring atom data (Sb and Ge respectively). Second, neither the Ge data nor the Sb data indicate the presence of Sb-Ge bonding. Finally, as we discuss below, bond counting exercises indicate that, within the error, the coordination numbers reported are consistent with a comprehensive amorphous model.

3. Discussion

Assuming the only like-atom bonds are Ge-Ge bonds, and $N_{\text{av}}(\text{Te}) = 2.4$, then 1/7 (~14%) of the Ge bonds are homopolar. This agrees, within the error, with the reported results for Ge-Ge bonding. Based on these EXAFS results, the presence of homopolar bonding of Ge suggests a model where *all* Ge atoms are bonded to one Ge atom and three Te atoms in a Ge_2Se_3 type local bonding arrangement [10], as shown in Fig 1. Sb atoms are then interspersed evenly throughout the structure with Te neighbors in Sb_2Te_3 arrangements.

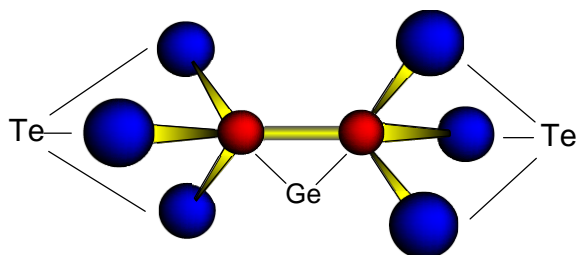


Fig. 1. Proposed Ge_2Te_3 configuration.

The existence of the second, short Sb-Te bond length raises questions regarding the nature of defects in the as-deposited material. Previously [11,12], this shortened length was attributed to an electrostatic, or dative [13] bond. A closer examination of the data suggests an alternate explanation for this bond. The bond length reported here (2.56 Å) is too short to be modeled by a homopolar Sb-Sb bond (~2.86 Å). It can, however, be associated with a bond between a positively charged Te^+ atom and a neutral Sb atom. By combining the covalent radius of 1.43 Å for Sb with a radius for Te^+ of 1.15 Å (estimated by interpolating between the ionic radii of Te^{-2} , Te^{+4} , Te^{+6} , and the covalent radius for neutral Te), the bond length between a positively charged Te^+ defect and a neutral Sb atom is estimated to be 2.58 ± 0.01 Å. This estimate is much closer to the measured bond length than either the Te-Te bond or the uncharged Te-Sb bond. A similar argument can be made to rule out the possibility that the measured shorter Ge-Ge bond length of 2.43 Å is a bond between a neutral Ge atom and a Te^+ ion, where the estimated length would then be 2.31 Å. The conclusion is that a three-fold coordinated Te with a short (~2.6 Å) Sb bond is the most likely explanation of the data.

Because GST is a neutral system, any positive charge gained by an overcoordinated Te atom must be balanced by the presence of a corresponding negative charge elsewhere in the system. These types of defects are usually referred to as Valence Alternation Pair defects, or VAPs [14]. It is likely that the negatively charged defect that is the conjugate pair partner to Te^+ is a negatively charged, two-fold coordinated Sb, i.e. Sb^- or a negatively charged, three-fold coordinated Ge, i.e. Ge^- . Because the results show, on average, an overcoordinated rather than an undercoordinated Sb atom, the presence of Sb^- ions can be ruled out. An ionic bond between Ge^- - Te^+ bond, however, would be indistinguishable (by EXAFS) from a covalent bond of the same species. It is assumed, then, that in order to satisfy the charge conservation constraint, it is the Ge atom that acquires the excess electron lost by the overcoordinated Te atom. Finally, because only ~4% of the Te atoms participate in the shorter Sb-Te bond, the corresponding feature in the Te EXAFS spectrum is too small to observe and analyze with any precision.

The physical requirement that the number of constraints in an amorphous material equals the number of degrees of freedom in the space that material occupies (or network dimensionality) defines a relatively simple criterion for an ideal, strain-free thin film or bulk material [4]. As the thin film materials addressed in this paper are neither i) one-dimensional or ii) two-dimensional and non-

planar networks, the latter bond constraint metric is three, so that the average number of bonds/atom C_{av} is given in Eq. (1),

$$C_{av} = 3 \quad (1)$$

This equation is the basis for discriminating between materials with different degrees of ideality in the context of the “ease of glass formation”. When it is met, a material may be considered to be a “good glass-former.” BCT’s subtlety manifests in determining the number of bonding constraints/atom in any given system.

For a system comprised of 2-, 3-, and 4-fold coordinated atoms with N atoms in its molecular formula, C_{av} can be written in terms of the stretching and bending constraints, f_s and f_b , respectively. If n_r is the number of atoms with r -fold coordination in one molecular unit and N is the total number of atoms in that unit, it follows that

$$C_{av} = \frac{1}{N} \sum_{r=2}^4 n_r (f_s + f_b). \quad (2)$$

From this equation, it can be shown [4] that

$$C_{av} = \frac{5}{2} \langle r \rangle - 3. \quad (3)$$

where $\langle r \rangle$ = the average coordination of the material. The condition that a material be a good glass former expressed in Eq. (1) is then equivalent to the condition that the average coordination be given by

$$\langle r \rangle = 2.4. \quad (4)$$

An alternate approach that arrives at the same conclusion (Eq. 4) is given by rigidity theory. Developed originally by LaGrange [6] and Clerk Maxwell [7], and later by Thorpe and co-workers [5], rigidity theory considers vibrational modes in systems with multiply-coordinated atoms in a material with local molecular units of N atoms. In calculating the total number of modes of vibration of such a system, they identify modes that require energy (i.e. constraints) and those that do not. The latter are the so-called zero-frequency or floppy modes, given the symbol F . F can be expressed as the difference between the total possible number of vibrational modes of the system, $3N$, and the modes determined by constraint counting. Thus, F is given by

$$F = 3N - \sum_{r=2}^4 n_r \left(\frac{r}{2} + [2r - 3] \right). \quad (5)$$

The fraction of zero-frequency modes, $f = F/3N$ may then be calculated using Eq. (2) and Eq. (3), and is given by:

$$f = 2 - \frac{5}{6} \langle r \rangle. \quad (6)$$

With increasing average network coordination, the fraction of zero frequency modes decreases, and is exactly equal to zero at the condition given by in Eq. (4). The

relationship between f and $\langle r \rangle$ is shown by the solid line of Fig. 2. The equivalence of the approach based on the assumption inherent in BCT (Eq. (1)) and the approach of rigidity theory (Eq. (6)) is manifest in the fact that each identify a material with $\langle r \rangle = 2.4$ as lying at a nexus dividing materials that are floppy from those that are stressed-rigid with respect to material properties.

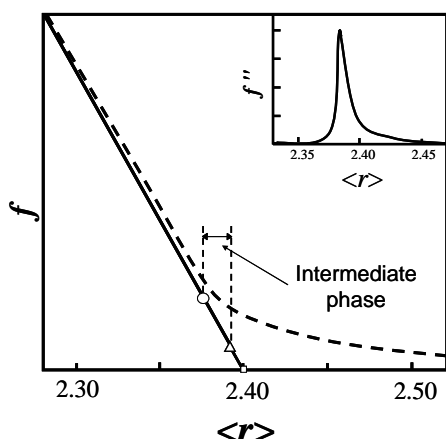


Fig. 2. Plot of f as a function of $\langle r \rangle$. Theory shown by solid line and model shown by dashed line. Inset shows second derivative of f as a function of $\langle r \rangle$. Figure adapted from Ref. 5.

Beyond the simple analytical treatment outlined above, this research also includes computer modeling of large networks of atoms, providing a numerical determination of the fraction of zero-frequency modes, f [15]. Plots of f as a function of $\langle r \rangle$ reveal three distinct composition regions. One such plot for a system of 2-, 3-, and 4-fold coordinated atoms is shown as the dashed line of Fig. 2. A transition region is readily identified in a plot of the second derivative of f with respect to $\langle r \rangle$. This is as shown in the inset of the figure, and it identifies a narrow transition region, $2.37 < \langle r \rangle < 2.44$, between floppy and stress-rigid regimes. The lower bound of this transition region represents the development of small and isolated pockets of rigid clusters, or *local rigidity*, the number of which increases as the average coordination increases. The upper bound indicates the percolation, or complete interconnection, of these locally rigid clusters, i.e., *global rigidity*, to generate a stressed-rigid material. For alloys with multiply-coordinated atoms such as $\text{Ge}_x\text{Sb}_y\text{Te}_{1-x-y}$ numerical modeling efforts such as this clearly identify three types of material with different values of C_{av} : i) a floppy a material with low average coordination; ii) a stressed-rigid material with high average coordination; and iii) an intermediate-phase material near $\langle r \rangle = 2.4$ that is an ideal locally stressed material without percolation of stress, or *unstressed rigid* material.

A generic ternary alloy diagram (Fig. 3a) provides a graphic representation of three distinct material regimes in a system such as GST. The vertices represent a 2-fold coordinated chalcogen, C; a three fold coordinated pnictogen, P, and a four-fold coordinated tetrahedrally coordinated atom T. The average coordination $\langle r \rangle$ ranges

from 2 to 4 as shown. For low coordination near the C vertex, the material is floppy and while glasses may be formed, they tend to have defects. In this corner of the diagram the locus of glass-forming compositions is indicated as the shaded region. Far removed from the C vertex, the material does not form glasses as indicated by the cross-hatched region. The system is locally too constrained to allow for glass formation. Between the two regions is a halo of material surrounding the glass-forming region.

The halo of Fig. 3a represents the locus of a class of materials that is distinct from either of the more extreme cases of under constrained (shaded) and over constrained (cross hatched) material. The existence of this class has been experimentally established by Boolchand and co-workers [16] who use Raman spectroscopy to identify the three regions of the alloy diagram. Using the terms “floppy”, “transition”, and “rigid”, they clearly identify a second-order phase transition from floppy to unstressed rigid (transition) material and a first-order transition from the transition material to the stressed rigid regime. These investigators identify these demarcations as rigidity transitions.

Fig. 3b shows the specific ternary alloy diagram for $\text{Ge}_x\text{Sb}_y\text{Te}_{1-x-y}$. Dashed tie lines link molecular solid compositions (GeTe and Ge_2Te_3 to Sb_2Te_3) that lie on the triangle’s sides. Intersections of these lines with the dash-dot bisector of the Te vertex represent the compositions $\text{Ge}_2\text{Sb}_2\text{Te}_5$ and $\text{Ge}_2\text{Sb}_2\text{Te}_6$, shown as the solid and open circles respectively.

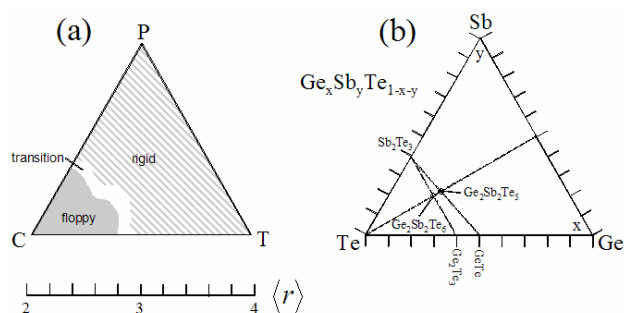


Fig. 3. Ternary alloy diagrams involving a chalcogen, a pnictogen, and a tetrahedrally coordinated material. (a) In general alloys may be considered floppy, rigid, or transitional. (b) In the GeSbTe system, $\text{Ge}_2\text{Sb}_2\text{Te}_5$ lies on the intersection of a tie line (connecting GeTe to Sb_2Te_3) and the bisector of the 60° angle at the Te vertex. Bond constraint theory and EXAFS results allow one to determine to which of the material ranges of figure (a) the alloys of figure (b) apply.

Calculating C_{av} for GST begins with analysis of the vibrational modes of the system. To zeroth order, a tetrahedral Ge configuration yields a C_{av} of 7. This is, however, too simplified, as bond-bending constraints can be removed by considering in detail the specific bond bending constraints around the Ge atom. The force constant for the Ge-Ge-Te bending motion is significantly reduced with respect to that of a Te-Ge-Te bending motion due to the different Ge-Ge-Te and Te-Ge-Te bond

energies. This permits the removal of 2.67 bending constraints for the Ge_2Te_3 arrangement. In the case of undercoordinated Ge, the bond order is increased from 1 to 4/3, and the constraints are removed proportionally [17], resulting in the same number of total retained constraints. The EXAFS results suggest a bonding model in which all Ge atoms are either in the Ge_2Sb_3 arrangement or an undercoordinated pyramidal GeTe_3 configuration, thus the total number of constraints around the average Ge atom is reduced from 7 (5 bending) to 4.33 (2.33 bending).

In the Sb system, there are 1.5 stretching constraints and 3 bending constraints, resulting in 4.5 total constraints. None of these constraints are broken; therefore, the total number of constraints around Sb atoms is 4.5.

The Te system raises a different sort of challenge. Table 1 shows that Te is over-coordinated, and the following simple bond-counting exercise supports this result. The proposed model gives $\text{Ge}_2\text{Sb}_2\text{Te}_5$ as a combination of Ge_2Te_3 and Sb_2Te_3 structural units. This counting results in a deficiency in Te for the GST composition, as stoichiometry requires that the addition of these two units equal $\text{Ge}_2\text{Sb}_2\text{Te}_6$. This 1/6 or ~17% Te deficiency is reflected in our results, as the percent of over-coordinated Te determined from these fits is $0.4/2.4 = \sim 17\%$. A Te deficiency, combined with 8-N coordination of Ge and Sb require that some Te atoms over-coordinate, resulting in the presence of both two-fold and planar-three-fold geometries. No constraints can be removed for the former configuration, and in the latter, the bond order is reduced from one electron/bond to 2/3 electrons/bond. As with Ge, constraints are removed for this configuration, but proportionally so, resulting in 2 constraints for planar-three-fold coordinated Te, as well as two-fold coordinated Te. Therefore the number of total constraints for all Te atoms is 2.

Table 1. Coordination numbers and nearest neighbor bond distances for $a\text{-Ge}_2\text{Sb}_2\text{Te}_5$ as determined by EXAFS. Internal consistency is manifest in identical values (within the error) for heteropolar bonding distances when using x-ray absorption data from either atomic species.

TABLE 1. Coordination numbers and interatomic distances for $\text{Ge}_2\text{Sb}_2\text{Te}_5$			
Atom	Bond	Coordination (N)	R(Å)
Ge	Ge-Te	3.9 ± 0.5	2.63 ± 0.01
	Ge-Ge	0.6 ± 0.2	2.47 ± 0.03
Sb	Sb-Te	2.8 ± 0.5	2.83 ± 0.01
	<i>Sb-Te(e)</i>	0.5 ± 0.3	2.51 ± 0.01
Te	Te-Ge	1.2 ± 0.3	2.62 ± 0.01
	Te-Sb	1.2 ± 0.3	2.83 ± 0.01

Using the numbers above, the average number of constraints for the $\text{Ge}_2\text{Sb}_2\text{Te}_5$ system is calculated as follows: Ge contribution: $4.33 \times 2 = 8.66$; Sb contribution: $4.5 \times 2 = 9$; Te contribution: $2 \times 5 = 10$. Thus,

$$C_{av} = \frac{8.66 + 9 + 10}{9} = 3.07.$$

This value of C_{av} nears the ideal value of 3 suggested for a material in the stress-free state, and more importantly, for a good glass former.

The value of C_{av} , is very close to three for the chemically ordered molecular structure, including the VAP defects. The significant departures from random alloy bonding, which reduce configurational entropy but prevent percolation of strain, indicate that the $\text{Ge}_2\text{Sb}_2\text{Te}_5$ as-deposited film is in an intermediate state. The durability of the transition results from a balance between the enthalpy and the entropy components of the free energy of GST. Because of this balance, repeated cycling is possible and the material neither locks into an enthalpy driven crystalline state nor does it settle into an entropy driven disordered network.

4. Conclusions

EXAFS studies of the nearest-neighbor bonding of Ge, Sb and Te in as-deposited $\text{Ge}_2\text{Sb}_2\text{Te}_5$ films are presented. Analysis of the Ge K spectrum indicates significant concentrations of both Ge-Ge and Ge-Te bonds. Additionally, concurrent analysis of the three EXAFS spectra yields internally self-consistent atomic coordination numbers and bond lengths. Combined with bond-energies for the system, the EXAFS results give the following molecular structure: $\text{Ge}_2\text{Sb}_2\text{Te}_5 = \text{Ge}_2\text{Te}_3 + \text{Sb}_2\text{Te}_3$, with i) 17% of the Te-atoms 3-fold, rather than 2-fold coordinated, ii) 25% of the Sb atoms participating in semi-ionic bonding with an overcoordinated Te^+ atom, and iii) charge conservation enabled through the inclusion of valence alternation pair defects in the form of negatively charged, two-fold coordinated Sb^- atoms. The over-coordinated Te-atoms are assumed to have a positive formal charge of 1, and a subsequently smaller atomic radius, thereby accounting for the reduced distance associated with the shortened Sb-Te bond. The average bond coordination, $\langle r \rangle$, and average number of bond-stretching and -bending constraints/atom, C_{av} , have been determined using bond constraint theory. The inclusion of Ge-Ge bonding in Ge_2Te_3 groups provides the microscopic basis for the good glass forming capability of GST and its propensity for repeatable phase change transitions.

Acknowledgements

Work supported by the Air Force Research laboratory under grant no. F29601-03-01-0229 and by the National Science Foundation under grant no. DMR 0307594. Use of the Advanced Photon Source was supported by the U. S. Department of Energy, Office of Science, Office of Basic Energy Sciences, under Contract No. W-31-109-ENG-38. MRCAT operations are supported by the Department of Energy and the MRCAT member institutions.

References

- [1] S. R. Ovshinsky, *Phys. Rev. Lett.* **20**, 1450 (1968).
- [2] S. Hudgens, B. Johnson, *MRS Bulletin*, 1, Nov. (2004).
- [3] A. V. Kolobov, P. Fons, A. I. Frenkel, A. L. Ankudinov, J. Tominaga, T. Uruga, *Nature Mater.* **3**, 703 (2004).
- [4] J. C. Phillips, *J. Non-Cryst. Solids* **34**, 153 (1979).
- [5] M. F. Thorpe, *J. Non-Cryst. Solids* **57**, 355 (1983).
- [6] J. L. LaGrange, *Mécanique Analytique*, Paris (1788).
- [7] J. C. Maxwell, *Philos. Mag.* **27**, 294-299 (1864).
- [8] D. A. Baker, *Phys. Rev. Lett.* **96**, 255501 (2006).
- [9] F. A. Cotton, G. Wilkinson, *Advanced Inorganic Chemistry*, 3rd Edition (Interscience Publishers, New York, 1972), Chap. 3, p. 117 (Table 3.4).
- [10] A. Feltz, *Amorphe und glasartige anorganische Festkörper*, (Akademi-Verlag, Berlin, (1983), p. 248.
- [11] D. A. Baker, XAFS 13 meeting, in press.
- [12] D. A. Baker, MRS Spring 2006 meeting, in press.
- [13] L. Pauling, *The Nature of the Chemical Bond*, 3rd Edition (Cornell University Press, 1960), p. 511.
- [14] M. Kastner, D. Adler, H. Fritzsche, *Phys. Rev. Lett.* **37**, 1504 (1976).
- [15] D. J. Jacobs, M. F. Thorpe, *Phys. Rev. Lett.* **75**, 22 (1995).
- [16] Xingwei Feng, W. J. Bresser, P. Boolchand, *Phys. Rev. Lett.* **78**, 23 (1997)
- [17] R. Kerner, J. C. Phillips, *Solid State Communications* **117**, 47 (2001).

[✉]Corresponding author: Michael_Paesler@ncsu.edu